Atractylodin ameliorates ovalbumin-induced asthma in a mouse model and exerts immunomodulatory effects on Th2 immunity and dendritic cell function

YU-CHAO LIN[1-3], CHING-CHIEH YANG[4-6], CHING-HSIUNG LIN[7], TE-CHUN HSIA[1-3], WEN-CHENG CHAO[8-10] and CHI-CHIEN LIN[11,12]

[1]Graduate Institute of Clinical Medical Science, Department of Medicine; [2]Department of Internal Medicine, Division of Pulmonary and Critical Care Medicine; [3]Department of Respiratory Therapy, China Medical University, Taichung 40402; [4]Department of Radiation Oncology, Chi-Mei Hospital, Tainan 71004; [5]Institute of Biomedical Sciences, Department of Science, National Sun Yat-Sen University, Kaohsiung 804; [6]Department of Pharmacy, Chia-Nan University of Pharmacy and Science, Tainan 71710; [7]Department of Internal Medicine, Division of Chest Medicine, Changhua Christian Hospital, Changhua 50006; Departments of [8]Critical Care Medicine and [9]Chest Medicine, Taichung Veterans General Hospital; [10]Department of Industrial Engineering and Enterprise Information, Tung Hai University, Taichung 40705; [11]Institute of Biomedical Science, Department of Life Sciences, The iEGG and Animal Biotechnology Center, National Chung-Hsing University, Taichung 40227; [12]Department of Medical Research, China Medical University Hospital, Taichung 40402, Taiwan, R.O.C.

Received October 15, 2019; Accepted August 11, 2020

DOI: 10.3892/mmr.2020.11569

Abstract. Asthma is a leading allergic disease worldwide, demonstrating an ever-increasing prevalence over the past two decades. Asthma is characterized by allergen-associated airway hyperresponsiveness (AHR) that primarily results from T helper 2 (Th2) cell inflammation, in which dendritic cells (DCs) serve an important role in determining T cell development after encountering an antigen. Atractylodin (ATL), a polyethene alkyne extracted from *Atractylodis rhizoma* (also known as Cangzhu), has proven effective in treating digestive disorders, rheumatic disease and influenza. In addition, ATL was discovered to alleviate mouse collagen-induced arthritis via regulating DC maturation. The present study aimed to investigate the effect of ATL on asthma given that DCs serve an essential role in Th2-mediated inflammation in asthma. Mouse model of asthma was induced by ovalbumin (OVA). OVA-induced airway hyperresponsiveness (AHR) and inflammatory cells in bronchoalveolar lavage fluid (BALF) were detected. The production of IgE and IgG1 in serum and cytokines in BALF were detected by ELISA. The effects of ATL on dendritic cells maturation and T cell expansion were detected by flow cytometry analysis and 3H-thymidine incorporation. Using a model of OVA-induced asthma, it was demonstrated that ATL ameliorated AHR and decreased the levels of IL-4, IL-5 and IL-13 in bronchoalveolar lavage fluid (BALF), and OVA-specific IgE and IgG1 in the serum. OVA-stimulated splenocytes were used to demonstrated that ATL decreased cell expansion and the production of IL-4, IL-5 and IL-13 in the culture medium. In order to determine the cellular mechanism of ATL in asthma, splenic DCs were isolated and it was subsequently observed that ATL downregulated the expression levels of CD40 and CD80. Furthermore, OVA-stimulated $CD4^+$ T cells were co-cultured with splenic DCs, which revealed that ATL-treated splenic DCs led to impaired cellular proliferation and the production of IL-4, IL-5 and IL-13 in OVA-stimulated T cells. In conclusion, these results indicated that ATL may suppress antigen-specific Th2 responses in an OVA-induced allergic asthma model via regulating DCs. Therefore, ATL may exhibit therapeutic potential in the management of asthma and other allergic diseases presenting with Th2 inflammation.

Correspondence to: Professor Chi-Chien Lin, Institute of Biomedical Science, Department of Life Sciences, The iEGG and Animal Biotechnology Center, National Chung-Hsing University, 145 Xingda Road, South, College of Life Sciences Building (Room 1208), Taichung 40227, Taiwan, R.O.C.
E-mail: lincc@dragon.nchu.edu.tw

Dr Wen-Cheng Chao, Department of Critical Care Medicine, Taichung Veterans General Hospital, 1650 Taiwan Boulevard Sect. 4, Taichung 40705, Taiwan, R.O.C.
E-mail: cwc081@hotmail.com

Key words: asthma, T helper 2 cells, dendritic cells, atractylodin, *Atractylodis rhizoma*

Introduction

Affecting ~350 million individuals worldwide in 2015, asthma is currently a major global health concern, with the global

prevalence of asthma increasing by 12.6% (95% CI, 9.0-16.4%) from 1990 to 2015 (1). Asthma is a complex inflammatory disorder of the airways and airway hyperresponsiveness (AHR) is a hallmark feature of asthma (2). Asthma had been considered to be a single disease for decades; however, previous studies have recognized distinct phenotypes among patients with asthma (3,4). Allergic asthma with high T helper 2 (Th2) inflammation is the primary phenotype among patients with asthma, and increasing novel biological agents have been developed that target Th2-associated cytokines, including IL-5 and IL4/13 (5). Dendritic cells (DCs) serve a pivotal role in determining T cell development after encountering an antigen, and a number of studies have demonstrated that DCs were crucial in the pathogenesis of asthma via inducing Th2 inflammation in response to allergens (6,7).

Atractylodis rhizoma (also known as Cangzhu), a traditional herbal medicine used to treat digestive disorders, rheumatic disease and influenza, consists of a number of essential components, including sesquiterpenes, phenolic acids and polyethene alkynes (8). Atractylodin (ATL), a polyethene alkyne extract, was discovered to ameliorate intestinal inflammation via regulating MAPK activation and alleviate acute lung injury via suppressing nucleotide-binding domain-like receptor protein 3 inflammasome and toll-like receptor 4 activation (9-12). Our recent study further demonstrated that ATL ameliorated mouse collagen-induced arthritis via regulating DC maturation (13).

Therefore, the present study aimed to investigate the impact of ALT on asthma, as DCs have been identified to serve an essential role in Th2 inflammation in asthma. An ovalbumin (OVA)-induced asthma mouse model was used to characterize the effect of ATL on AHR, as well as the production of Th2-associated cytokines and OVA-specific IgE. The model was also used to evaluate the impact of ATL on the cellular proliferation and cytokine production of OVA-specific T cells, and to determine how ATL affected the maturation of DCs. The results provided evidence of the therapeutic effect of the i.p. injection of ATL on the maturation of DCs and downstream Th2 inflammation in asthma, and indicated a potential application of ATL for treating patients with asthma and high Th2 inflammatory levels.

Materials and methods

Animals and experimental design. A total of 24 six-week-old male BALB/c mice (weight, 18-22 g), were obtained from the National Laboratory Animal Center. The mice were placed in sterile cages under a regulated temperature (22±3˚C), humidity (55±5%) and 12-h day/night cycle conditions and *ad libitum* access to sterilized mouse chow and water. Ethical approval for the present study was obtained from the Institutional Animal Care and Use Committee (IACUC) of National Chung-Hsing University (Taichung, Taiwan; approval no. IACUC 108-072). Experiments were performed in accordance with relevant guidelines for Guide for the Care and Use of Laboratory Animals, 8th edition (14). In order to investigate the protective effects of ATL on asthma in mice, the 24 male BALB/c mice were randomly divided into four groups (n=6 per group): i) normal control (NC; vehicle), containing mice which were not challenged with OVA (Thermo Fisher Scientific, Inc.) and received daily intraperitoneal injection (i.p.) injection equal volumes of vehicle (10% DMSO (ChemCruz; Santa Cruz Biotechnology, Inc.) and 90% glyceryl trioctanoate (Sigma-Aldrich; Merck KGaA); ii) OVA group, in which mice were stimulated with OVA and received equal volumes of vehicle; iii) OVA/ATL 20 group, in which mice were stimulated with OVA and received 20 mg/kg ATL (National Institute for Food and Drug Control); and iv) OVA/ATL 40 group, in which mice were stimulated with OVA and received 40 mg/kg ATL. The single daily dose of ATL was administered via i.p. injection for 16 days starting on day 15 of primary immunization (Fig. 1A). The dosage and administration frequency were implemented based on previous studies (12,13,15). The OVA-immunized mice received 20 μg OVA (i.p.) and 2% alum adjuvant (InvivoGen) dissolved in saline (final volume, 200 μl) on days 1, 7 and 14. These mice were then challenged with 5% OVA in 0.9% NaCl by inhalation for 30 min daily for 5 consecutive days (days 27-31). On day 32, the AHR of each mouse was measured as described below. Finally, on day 33, mice were sacrificed using carbon dioxide (air displacement rate, 30% of the chamber volume/min). Mice were exposed to 50% CO_2 until they were unconscious and experienced cardiac arrest.

Measurement of AHR via unrestrained whole-body plethysmography. On day 32, AHR was measured via methacholine (Mch; Sigma-Aldrich; Merck KGaA)-induced airflow obstruction in conscious unrestrained mice placed in a whole-body plethysmograph (Buxco; Data Sciences International; Harvard Bioscience, Inc.). Pulmonary resistance was evaluated and expressed as enhanced pause. Briefly, mice were first exposed to aerosolized 1X PBS [0.8% NaCl, 0.02% KH_2PO_4, 0.115% Na_2HPO_4, 0.02% KCl [pH 7.4]), then challenged with a series of aerosolized Mch (3.125-50 mg/ml) with an ultrasonic nebulizer over the recording time period. Each nebulization lasted for 3 min and records were taken for 3 min after nebulization. Every aerosol was separated by a 15-min recovery period in order to allow airway Penh to return to the baseline level.

Collection and analysis of bronchoalveolar lavage fluid (BALF). On day 33, mice were sacrificed and placed in a supine position. The trachea was surgically exposed and cannulated with catheters pointing towards the lungs. The BALF was obtained by instilling two 1-ml aliquots of PBS via the catheter followed by 2 aspirations of BALF into the 1 ml syringe. The obtained BALF was centrifuged at 3,420 x g at 4˚C for 5 min and the supernatants were stored at -80˚C for further experiments.

The levels of cytokines in the BALF supernatant, including IL-4 (cat. no. 88-7044-77), IL-5 (cat. no. 88-7054-22), IL-13 (cat. no. 88-7137-88) and TNF-α (cat. no. 88-7324-22), were analyzed using ELISAs (eBioscience; Thermo Fisher Scientific, Inc.) according to the manufacturer's instructions.

Furthermore, cell pellets from the BALF were resuspended in 200 μl saline. Then, 100 μl cell suspension was mixed with 0.4% trypan blue solution for ~3 min at room temperature to determine total cell counts using a hemocytometer (Neubauer-improved; Paul Marienfeld GmbH & Co. KG).

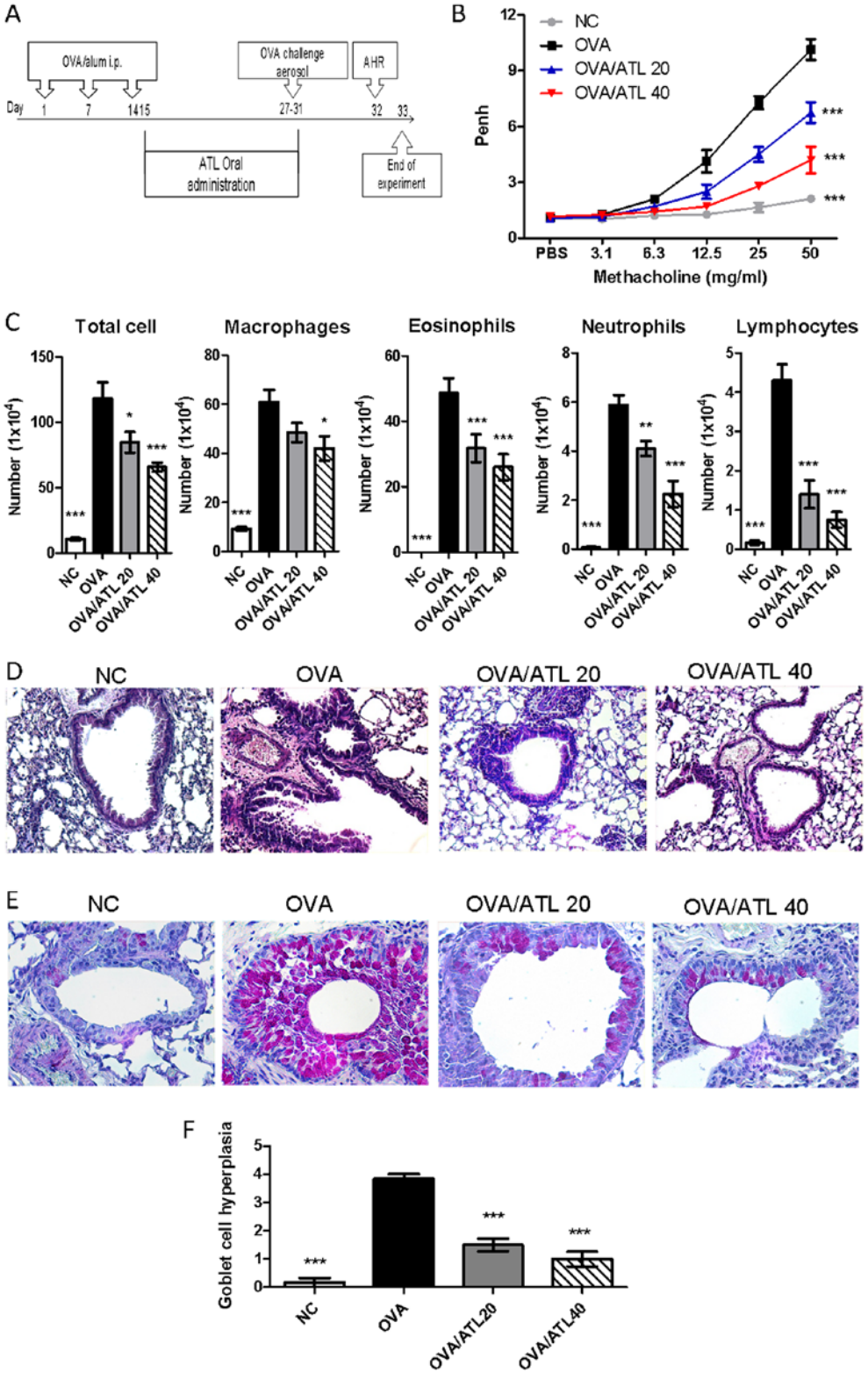

Figure 1. Effect of ATL on AHR and airway inflammation. (A) Experimental procedure. BALB/c mice were randomized into four groups (n=6 mice per group). NC mice were not sensitized with OVA or treated with ATL. On days 1, 7 and 14, OVA, OVA/ATL 20 and OVA/ATL 40 groups were sensitized via i.p. injection of OVA allergen. OVA/ATL 20 and OVA/ATL 40 mice were i.p. injected daily with 20 and 40 mg/kg ATL, respectively, on days 15-31. Finally, mice in all 4 groups were exposed to OVA aerosols on day 27-31, and AHR was measured on day 32. BALF, serum, lung and spleen tissue were collected. (B) Effect of ATL on AHR levels. Mice inhaled increasing doses of methacholine (3.125-50 mg/ml). Penh levels represent the degree of AHR. ***P<0.001 vs. OVA. (C) Mice treated with ATL exhibited decreased cell counts in the BALF. Total cells, macrophages, eosinophils, lymphocytes and neutrophils were counted following Diff-Quik staining. Histological examination of lung sections stained with (D) Hematoxylin and eosin to examine inflammatory cell infiltration and (E) periodic acid-Schiff staining to examine goblet cell hyperplasia and mucus secretion (magnification, x400 for both). (F) For the semi-quantification of goblet cell hyperplasia, slides were examined in a double-blind setting using a semi-quantitative scoring system. A scored scale from grade 0 to 4 was implemented depending on the percentage of goblet cells in the epithelium: grade 0 (no goblet cells); grade 1 (<25%), grade 2 (25-50%), grade 3 (51-75%) and grade 4 (>75%). The mean goblet cell hyperplasia score was then calculated for each mouse. Data are presented as the mean ± SEM of six mice per group. *P<0.05, **P<0.01, ***P<0.001 vs. OVA. ATL, atractylodin; AHR, airway hyperresponsiveness; NC, normal control; OVA, ovalbumin; BALF, bronchoalveolar lavage fluid; Penh, enhanced pause.

The remaining 100 μl BALF was used to prepare CytospinR slides (Thermo Shandon Inc.). Briefly, samples were centrifuged at 30 x g for 6 min at 4˚C and the deposited cells were fixed to the microscope slides with 95% alcohol for 30 sec at room temperature, and then stained with 1X Diff-Quik solution (cat. no. 38721; Sysmex) for 30 sec at room temperature and visualized under a light microscope (magnification, x200). In each case, 10 randomly chosen high-power fields were selected from the CytospinR slides. Then, 200 cells were counted, and the percentage of each type of cell was calculated. White blood cells were classified as eosinophils, neutrophils, macrophages and lymphocytes based on cellular staining and morphological characteristics.

Lung histology study. Following lavage via trachea with sterile saline, lungs were immediately removed and fixed in 10% v/v buffered formalin (diluted in 0.01 mol/l PBS; pH 7.2) for 15 min at room temperature. Pulmonary tissues were subsequently sliced, embedded in paraffin and cut into 5-μm-thick sections. These paraffin sections were stained with hematoxylin for 10 min and eosin (H&E; Merck Millipore) for 5 min at room temperature or 0.5% periodic acid-Schiff stain (ScyTek Laboratories, Inc.) for 5 min at room temperature to evaluate inflammatory cell infiltration and goblet cell hyperplasia, respectively. Light microscopy (x200 magnification) was used for histopathological assessment. For the semi-quantification of goblet cell hyperplasia, slides were examined in a double-blind setting using a semi-quantitative scoring system as previously described (16,17) with certain modifications. Briefly, pathological changes were evaluated according to the modified 5-point scoring system (grade 0-4) and were expressed by score according to the percentage of the goblet cells in the epithelium: 0 (no goblet cells), 1 (<25%), 2 (25-50%), 3 (51-75%) and 4 (>75%). The mean goblet cell hyperplasia score was then calculated for each mouse in each group.

Detection of serum OVA-specific IgE and IgG1. A total of 700-1,000 μl mouse blood were collected from the submandibular vein on days 1, 21 and 33, which were allowed to coagulate for 1 h at room temperature. Following centrifugation at 1,000 x g for 10 min at 4˚C, the serum samples were stored at -80˚C until further analysis; all samples were thawed no more than twice. OVA-specific IgE and IgG1 levels in the mouse serum were analyzed via ELISAs. Briefly, 200 μg OVA diluted in 0.1 M $NaHCO_3$ (pH 9.6) was used to coat the 96-well microplates at 4˚C overnight. After washing with 1X PBS and blocking with 1% BSA (Sigma-Aldrich; Merck KGaA) in 1X PBS, diluted sera (1:5 for IgE and 1:2,000 for IgG1) in blocking buffer were added to the wells for overnight incubation at 4˚C. The following day, the plates were washed and incubated with horseradish peroxidase-conjugated rat anti-mouse IgE (1:5,000; clone no. LO-ME-3; cat. no. GTX761169; GeneTex, Inc.) or goat anti-mouse IgG1 (1:5,000; cat. no. ab97240; Abcam) antibodies at 4˚C overnight. After washing the well six times with 1X PBS to remove the unbound antibody. Then, 3,3',5,5'-tetramethylbenzidine (cat. no. 00-4201; Sigma-Aldrich; Merck KGaA) was added and incubated at room temperature for 15 min, and the absorbance at 450 nm was measured using an ELISA reader (Sunrise; Tecan Group Ltd.).

OVA-specific splenocyte responses. Mouse spleens from each treated group were collected immediately following sacrifice on day 33, and a single-cell suspension of splenocytes for OVA-specific cell proliferation and cytokine tests were obtained via repeatedly pressing the spleens with sterile 50-mesh stainless meshes and plungers as previously described (18). Then, the cells ($2x10^6$) were stimulated with 100 μg/ml OVA in complete RPMI-1640 medium (Gibco; Thermo Fisher Scientific) for 72 h in humidified incubator at 37˚C with 5% CO_2. The OVA-specific cell proliferation responses were quantified via incorporation of radiolabeled [3H] thymidine with specific activities of 1Ci (3.7 GBq) per well in humidified incubator at 37˚C with 5% CO_2 for 18 h. After labelling, cells were precipitated twice with ice-cold 10% trichloroacetic acid (TCA) 30 min at RT each, to remove acid soluble materials and then solubilized overnight in 1.0 M NaOH. The sample was then transferred into a scintillation vial and the radioactivity was measured via liquid scintillation counting β-Counter (Beckman Coulter, Inc.). The readout is radiation counts per minute (cpm) per well.

Additionally, centrifugation was performed at 1,000 x g for 15 min at 4˚C, the supernatant from the culture system of cells was collected to measure cytokine concentrations, including mouse IL-4, IL-5 and IL-13 levels, via standard sandwich ELISAs (eBioscience; Thermo Fisher Scientific, Inc.), according to the manufacturer's protocol.

Flow cytometric analysis of DC surface markers in vivo. On day 33, splenocytes from each treated group were extracted and fixed in 100 μl 2% formaldehyde (Sigma-Aldrich; Merck KGaA) in PBS buffer (pH 7.4) for 15 min at 4˚C and washed twice with 1 ml PBS followed by centrifugation of 400 x g for 5 min at 4˚C. Fixed cells were then blocked in 2% BSA/PBS for 15 min at 4˚C and resuspended in 50 μl staining buffer (PBS containing 2.00% FCS and 0.05% sodium azide). Subsequently, the cells were surface stained with FITC-conjugated mouse anti-CD11c (1:100; cat. no. 117306, clone no. N418; BioLegend, Inc.), phycoerythrin (PE)-anti-CD40 (1:100; cat. no. 124610, clone no. 3/23; BioLegend, Inc.) and PE-CD80 antibodies (1:100; cat. no. 104708, clone no. 16-10A1; BioLegend, Inc.) for 30 min at 4˚C. Isotype-matched, PE Rat IgG2a, λ Isotype Ctrl Antibody (1:100 dilution, cat. no. 402304, clone no. G0C3C12; BioLegend, Inc.) and PE Armenian Hamster IgG Isotype Ctrl Antibody (1:100 dilution, cat. no. 400908, clone no. HTK888; BioLegend, Inc.) were stained for 30 min at 4˚C and used for negative staining. CD40 and CD80 fluorescence intensity was measured using an BD Accuri™ 5 flow cytometer (BD Biosciences). Events were acquired with a forward side scatter threshold of 80,000 and a live gate on CD11c-positive events. The mean fluorescence intensity was calculated using BD Accuri™ C6 system software (CFlow version 1.0.264.15; BD Biosciences).

Isolation of CD11c(+) DCs. On day 33, splenocytes were collected. CD11c(+) DCs were positively selected using mouse CD11c MicroBeads UltraPure (cat. no. 130-125-835) and LS separation columns (both Miltenyi Biotec, Inc.), according to the manufacturer's instructions. Purified CD11c cells were determined via forward and side scatter and gated according to the size and granular characteristics of DCs. Based on flow

cytometry staining with FITC-conjugated mouse anti-CD11c, CD11c(+) DCs were found to be >80% pure (Fig. S1).

Reverse transcription-quantitative (RT-q)PCR. Total RNA was extracted from purified CD11c(+) DCs using TRIzol® reagent (Invitrogen; Thermo Fisher Scientific, Inc.), as previously described (19). RNA concentration was measured spectrophotometrically at 260 nm (A260) and 2 μg RNA was reverse transcribed into cDNA using an Applied Biosystems 2720 Thermal cycler (Thermo Fisher Scientific, Inc.) along with the following reagents: Moloney murine leukemia virus (MMLV) reverse transcriptase, 5X reaction buffer, dNTPs, RNAasin (RNase inhibitor) and oligo (dT) 15 primers (Promega Corporation). Briefly, primer annealing was initiated at 70˚C for 5 min followed by the addition of MMLV reverse transcriptase at 37˚C for 60 min. The reverse transcription reaction was terminated following heating to 72˚C for 10 min.

qPCR was subsequently performed using a Fast SYBR™ Green Master Mix (Applied Biosystems; Thermo Fisher Scientific, Inc.) on an ABI 7500 Fast Real-Time system (Applied Biosystems; Thermo Fisher Scientific, Inc.), according to the manufacturer's protocol. The following thermocycling conditions were used for the qPCR: Initial denaturation at 95˚C for 10 min; annealing and extension, 95˚C for 10 sec and 60˚C for 30 sec for 40 cycles. The following primers sequences were used (Tri-I Biotech, Inc.): IL-4 forward, 5'-TTTGAACGAGGTCACAGGAGAAG-3' and reverse, 5'-AGGACGTTTGGCACATCCA-3'; IL-12 forward, 5'-GCCAGTACACCTGCCACAAA-3' and reverse, 5'-TGTGGAGCAGCAGATGTGAGT-3'; and hypoxanthine guanine phosphoribosyl transferase 1 (HPRT) forward, 5'-GTTGGATAAGGCCAGACTTTGTTG-3' and reverse, 5'-GATTCAACTTGCGCCATCTTAGGC-3'. Quantification of the expression levels of the IL-4 and IL-12 genes in the samples was accomplished by measuring the fractional cycle numbers at which the expression levels reached a fixed threshold (Cq). The relative gene expression levels were calculated via the $2^{-\Delta\Delta Cq}$ method (20), using the constitutively expressed gene, HPRT, as a control for normalization. Data are expressed as n-fold relative to the NC group.

In vitro DC functional assays. In order to measure antigen-specific $CD4^+$ T cell proliferation and Th2 cytokine production, $CD4^+$ T cells were used to assay the antigen presenting capacity of CD11c(+) DCs. Briefly, the EasySep™ Mouse CD4 Positive Selection kit (Stemcell Technologies, Inc.) is used to isolate CD4(+) cells from single-cell suspensions of spleen, according to the manufacturer's protocol. Enriched $CD4^+$ T cells were co-cultured with enriched CD11c(+) DCs generated from the spleens of different groups of mice at a 2:1 DC: $CD4^+$ T cell ratio in RPMI-1640 medium supplemented with 10 % fetal bovine serum, 100 U/ml penicillin-streptomycin (both Gibco; Thermo Fisher Scientific, Inc.) and 50 μM β-mercaptoethanol (Sigma-Aldrich; Merck KGaA) for 96 h in humidified incubator at 37˚C with 5% CO_2, and cell proliferation was assayed via ^{3}HTdR incorporation as aforementioned.

In addition, DC/$CD4^+$ T cell culture supernatants were collected after 96 h by centrifugation of 400 x g for 5 min at 4˚C, and IL-4, IL-5 and IL-13 production levels were measured via ELISA kits (eBioscience; Thermo Fisher Scientific, Inc.).

Statistical analysis. The data are expressed as the mean ± SEM of three independent experiments. A Kruskal Wallis and Dunn's post hoc test, or one- or two-way ANOVAs and a Tukey's post hoc test were used to compare multiple experimental groups with GraphPad Prism software (version 5.0; GraphPad Software, Inc.). $P<0.05$ was considered to indicate a statistically significant difference.

Results

ATL decreases OVA-induced AHR and airway inflammation. The anti-allergenic effect of ATL was investigated in an OVA-induced asthmatic animal model. The experimental procedure for the treatment is presented in Fig. 1A. To investigate the therapeutic effect of ATL on asthma, AHR and inflammatory cell infiltration in the lungs were analyzed. Following the exposure to increasing concentrations of Mch (3.125-50 mg/ml), the degree of AHR was significantly increased in the OVA group compared with the NC mice, whereas treatment with 20 and 40 mg/kg ATL significantly decreased the response to Mch in a dose-dependent manner compared with the OVA group (Fig. 1B). In addition, there was a significantly increased number of inflammatory cells (including total cells, macrophages, eosinophils, neutrophils and lymphocytes) in the BALF from the OVA group compared with the NC group (Figs. 1C and S2). However, the influx of inflammatory cells in the OVA/ATL 20 and OVA/40 groups was significantly decreased compared with the OVA group (Figs. 1C and S2). Next, the effect of ATL on inflammatory cell influx was determined using H&E staining. The degree of inflammatory cells around the bronchioles was notably elevated in OVA-exposed mice compared with the NC group (Fig. 1D). However, in mice receiving 20 and 40 mg/kg ATL, the level of inflammatory infiltration was decreased (Fig. 1D). Moreover, a significant increase was observed in the number of goblet cells and mucus overproduction, which was indicated by a violet color, in the bronchial airways of the OVA group compared with the NC group (Fig. 1E and F). The ATL-treated groups did not exhibit notable changes in mucus production compared with the NC group (Fig. 1E and F). However, a significant reduction in the number of goblet cells was observed in both the OVA/ATL 20 and OVA/ATL 40 group compared with the OVA group. Collectively, these data indicated that ATL may attenuate OVA-induced allergic airway inflammation in mice.

ATL suppresses the production of OVA-induced Th2 cytokines in the BALF. BALF from the OVA group exhibited significantly elevated levels of typical Th2 cytokines, including IL-4, IL-5 and IL-13, and the proinflammatory cytokine, TNF-α, compared with the NC group (Fig. 2). However, IL-4, IL-5 and IL-13 levels in the BALF of OVA-sensitized mice were significantly decreased following the treatment with 20 or 40 mg/kg ATL, while TNF-α levels were only significantly decreased following the treatment with 40 mg/kg ATL. Collectively, these findings indicated that ATL modulated the magnitude of Th2-mediated cytokine expression levels of BALF during the development of OVA-induced allergic asthma.

ATL decreases OVA-specific antibody levels in the serum and T cell expansion in the spleen. Allergic asthma is recognized

as a Th2-dependent immune response with increased serum antigen-specific IgE and IgG1 production (21). In order to investigate the potential mechanism of ATL-induced inhibition of airway inflammation, the effect of ATL on the changes of serum IgE and IgG1 levels was evaluated. OVA challenge in sensitized mice induced a significant increase in serum OVA-specific IgE and IgG1 levels on days 21 and 33 (Fig. 3) compared with the NC group. However, 40 mg/kg ATL significantly inhibited Th2-dependent IgE and IgG1 expression levels compared with OVA group on day 21 (Fig. 3). In addition, both 20 and 40 mg/kg ATL significantly suppressed IgE and IgG1 levels on day 33. The high dose of ATL (OVA/ATL 40) exhibited a greater suppressive effect than the medium dose (OVA/ATL 20) on both IgE and IgG1 levels (Fig. 3).

To further investigate the effect of ATL on Th2 cell responses, splenocytes from the different groups of mice were stimulated *ex vivo* with OVA protein for 72 h. Following stimulation with OVA, ELISAs demonstrated that the splenocyte culture supernatants from OVA/ATL 20 and OVA/ATL 40 groups exhibited a significantly decreased production of Th2 cytokines, including IL-4, IL-5 and IL-13, compared with the splenocytes from the OVA group (Fig. 4A). In addition, decreased OVA-stimulated splenocyte proliferation was also found in OVA/ATL 20 and OVA/ATL 40 groups compared with the OVA group (Fig. 4B). Taken together, these results indicated the potential specific inhibition of the antigen specific Th2 response by ATL in a murine asthmatic model.

ATL decreases the capacity of spleen-enriched DCs to stimulate OVA-specific T cell activation in vitro. Antigen presenting cells, such as DCs, previously served an important role in the regulation of T cell-mediated immune responses in an OVA-induced asthma model (6,7). Our previous study also demonstrated that ATL modulated the lipopolysaccharide-induced maturation of mouse bone marrow DCs and suppressed the capacity of DCs to stimulate the T cell response (13). Thus, to further elucidate the cellular mechanism of ATL treatment on OVA-induced allergic asthma in mice, the phenotype and function of DCs obtained from the spleens were characterized. The treatment with 40 mg/kg ATL resulted in the sigsup (Fig. 5A and B). Consistent with the activated phenotype, OVA challenge in sensitized mice induced a significant increase in IL-4 expression levels of DCs compared with the NC group. However, DCs from the spleens of mice in the OVA/ATL 40 group had significantly downregulated expression levels of IL-4 (Fig. 5C) compared with OVA group, which serves a critical role in the induction of the Th2 immune response (5). However, no significant differences in Th1 cytokine IL-12 expression levels were noted between groups.

The potency of purified splenic CD11c(+)-enriched cells isolated to stimulate allogeneic OVA-stimulated T cell proliferation and cytokine production was compared between the different groups. CD11c(+) DCs from mice treated with 40 mg/kg ATL significantly decreased $CD4^+$ T cell proliferation (Fig. 5D) and decreased Th2 responses (IL-4, IL-5, IL-13; Fig. 5E) compared with CD11c(+) cells obtained from OVA mice. The OVA/ATL 20 group exhibited significantly inhibited IL-4 and IL-13 expression levels (Fig. 5E) but T cell proliferation (Fig. 5D) and the IL-5 expression levels (Fig. 5E) were

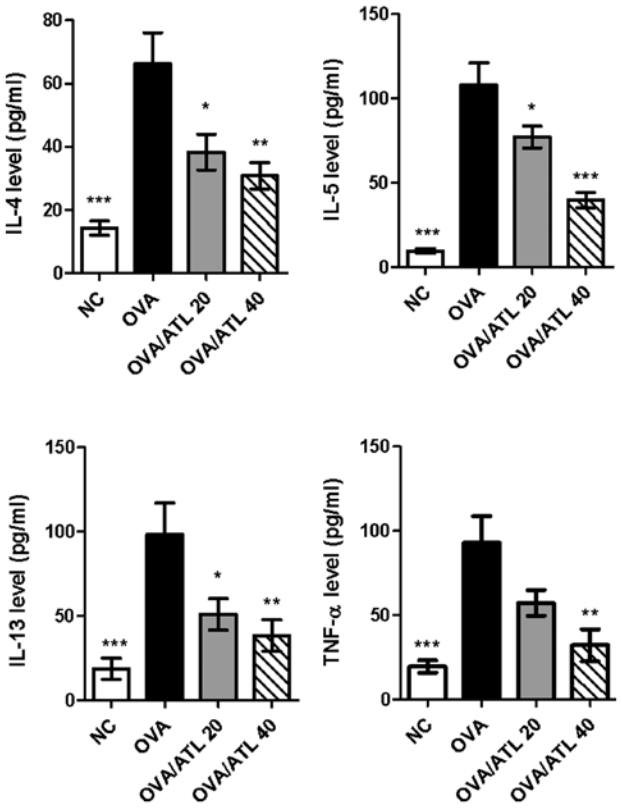

Figure 2. Effect of ATL on cytokine production levels in BALF. IL-4, IL-5, IL-13 and TNF-α levels in BALF were determined using ELISA kits. Data are presented as the mean ± SEM (n=6 mice per group). *P<0.05, **P<0.01, ***P<0.001 vs. OVA. ATL, atractylodin; BALF, bronchoalveolar lavage fluid; NC, normal control; OVA, ovalbumin.

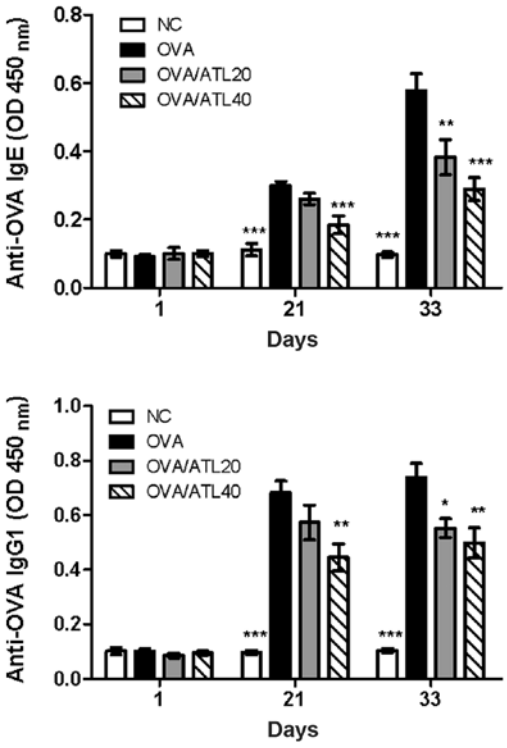

Figure 3. Effect of ATL on serum IgE and IgG1 levels. Serum OVA-specific IgE and IgG1 levels on days 1, 21 and 33 were analyzed via ELISA kits. The absorbance was measured at 450 nm with a microplate reader. *P<0.05, **P<0.01, ***P<0.001 vs. OVA. ATL, atractylodin; OVA, ovalbumin; NC, normal control.

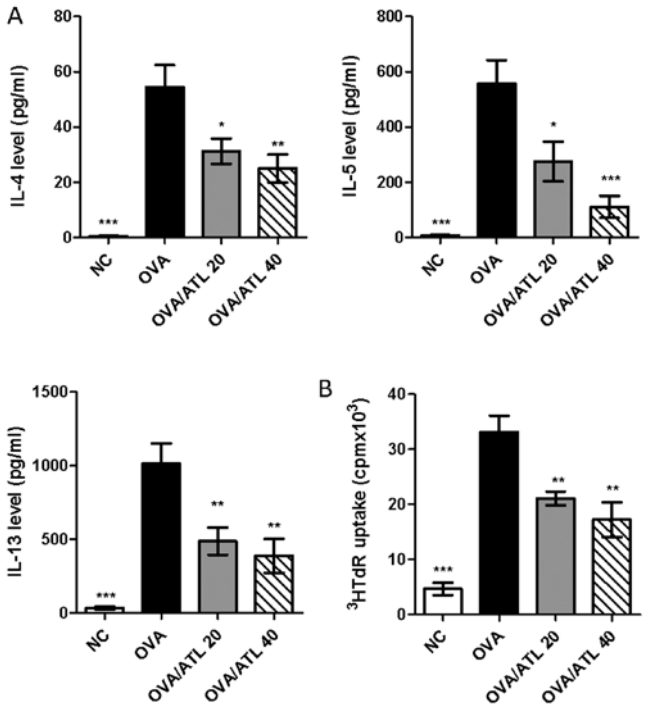

Figure 4. Effect of ATL on levels of cytokine production and proliferation in OVA-stimulated splenocytes. (A) Splenocytes from treated mice in each group were stimulated with OVA (20 μg/ml) for 72 h. IL-4, IL-5 and IL-13 levels in the supernatant were determined using ELISA kits. (B) OVA-specific T cell proliferation is decreased in ATL-treated mice. Splenocytes were stimulated with OVA for 72 h, then ith ^{3}HRdR was added for 18 h. The cpm values were measured via a liquid scintillation counting β-counter. Data are presented as the mean ± SEM (n=6 mice per group). The absorbance was measured at 450 nm with a microplate reader. *P<0.05, **P<0.01, ***P<0.001 vs. OVA group. ATL, atractylodin; OVA, ovalbumin; cpm, counts per minute; NC, normal control; ^{3}HRdR, [3H]-thymidine.

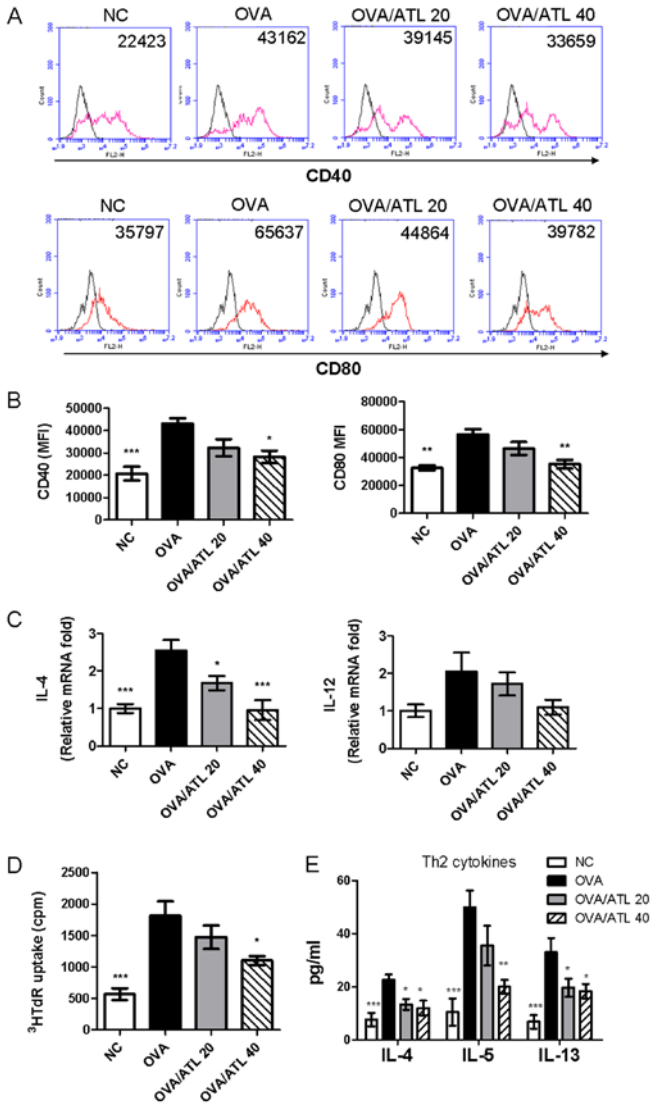

Figure 5. Treatment with ATL inhibits the expression levels of costimulatory molecules on splenic DCs. (A) CD40 and CD80 expression levels on splenic DCs were analyzed by flow cytometry. (B) Expression levels of activation markers are presented as MFI. (C) IL-4 and IL-12 mRNA expression levels were detected in purified splenic CD11c(+) DCs via reverse transcription-quantitative PCR. Data were normalized to hypoxanthine guanine phosphoribosyl transferase 1 expression levels. To determine the effect of splenic CD11c(+) DCs on the OVA antigen-stimulated T cell response, purified CD11c(+) DCs were co-cultured with CD4$^+$ T cells from OVA-immunized mice and the (D) proliferative capacity and (E) Th2 cytokine (IL-4, IL-5 and IL-13) production were measured. Data are presented as the mean ± SEM (n=6 mice per group) The absorbance was measured at 450 nm with a microplate reader. *P<0.05, **P< 0.01, ***P<0.001 vs. OVA group. ATL, atractylodin; DC, dendritic cell; MFI, mean fluorescence intensity; OVA, ovalbumin; NC, normal control; ^{3}HRdR, [3H]-thymidine; cpm, counts per minute; Th2, T helper 2 cell.

not significantly altered. These results indicated that high dose of ATL (OVA/ATL 40) modulation of DC function *in vivo* may serve an important role in the suppression of antigen-specific Th2 responses in an OVA-induced allergic asthma model.

Discussion

In the present study, an OVA-induced mouse model, characterized by OVA- induced AHR and allergic airway inflammation, was used to demonstrate the therapeutic potential of ATL in the management of asthma. The results showed that ATL may ameliorate OVA-induced AHR and Th2 inflammation via regulating the maturation of DCs in OVA-induced allergic asthma. ATL alleviated AHR, decreased the levels of Th2-associated cytokines, including IL-4, IL-5 and IL-13, in the lung and decreased the production of OVA-specific IgG1 and IgE. OVA-stimulated splenocytes were used to demonstrate that ATL decreased OVA-specific T cell proliferation and cytokine production. Furthermore, splenic DCs from OVA-stimulated mice were isolated to determine the regulatory effect of ATL on the expression levels of costimulatory molecules and OVA-specific T cells were co-cultured with splenic DCs to demonstrate the regulatory effect of ATL on DCs. The present results indicated the potential application of the i.p. injection of ATL in patients with asthma with high Th2 inflammatory levels.

Phytochemicals possess numerous pharmacological activities, including antioxidative, anti-inflammatory, anti-rheumatic, antimicrobial and anticancer effects (22,23). ATL, a phytochemical extracted from *Atractylodis rhizoma*, has exhibited anti-inflammatory effects in a number of diseases, including intestinal inflammation, rheumatic disease and influenza (9,10). Our previous study reported the effect of the i.p. injection of ATL on arthritis using a

mouse collagen-induced arthritis model; ATL alleviated the severity of disease progression, including paw swelling, clinical arthritis scores and pathological changes in joint tissues, and suppressed both the Th1 and Th17 pathways (13). In addition, ATL downregulated CD40, CD80 and CD86 expression levels in splenic DCs (13). The present study further demonstrated that the i.p. injection of ATL effectively suppressed DC maturation and downstream Th2 inflammation in asthma. Collectively, these results highlighted the potential role of ATL as an anti-inflammatory medication in diseases, including arthritis and asthma.

Asthma is a complex inflammatory disease, and the heterogeneity of airway inflammation indicates that distinct mechanisms may be involved (3). Among the increasing number of methods used for the identification of phenotypes among asthmatics, phenotyping via examining inflammatory cells in induced sputum is currently a practical method (4,24). It is estimated that ~30% of asthmatics have high levels of sputum neutrophils instead of eosinophilia, and the control of asthma in patients with neutrophilic airway inflammation is poor under standard inhaled corticosteroid treatment (4). Using endobronchial tissue gene expression levels analysis in patients with asthma, Choy *et al* (25) reported that the Th17 pathway was implicated in neutrophilic airway inflammation in asthma. However, there are heterogeneous phenotypes in patients with asthma, and the majority of current mouse models of asthma mimic eosinophilic asthma using numerous allergens, including OVA and house dust mite and cockroach allergens (26). As only OVA-induced asthma was used in the present study, the impact of ATL on pathways other than Th2 inflammation remains to be elucidated by other models mimicking neutrophilic asthma (27). However, our previous study reported that ATL affected the Th17 pathway in a collagen-induced arthritis mouse model.

In the past decade, a number of novel biological agents have been developed in addition to use of a monoclonal antibody targeting IgE for the management of patients with asthma and other atopic diseases, including atopic dermatitis and allergic rhinitis; these biological agents primarily target downstream cytokines, including IL-5 and IL-4/13 (5). The immunological pathways of IL-5, IL-4 and IL-13 are associated with DCs during the inflammatory reaction in the immunological networks of asthma: IL-4 enhances the capacity of DCs to stimulate the T cell secretion of Th2 cytokines IL-5 is implicated in the maturation of DCs, and IL-13 enhances the capacity of DCs to regulate the T cell secretion of IFN-γ (28,29). Furthermore, IL-4/IL-13 may increase the antigen uptake of DCs and cell migration into lymph nodes, wherein DCs prime the differentiation of naive T cells into Th2 cells (30). Additionally, IL-4 drives B cell class switching to the production of IgE (31). As illustrated *in vivo* and *ex vivo* in the present study, ATL regulated the upstream antigen presenting function of DCs; therefore, IL-4, IL-5, IL-13, IgG1 and IgE levels were also discovered to be decreased following the administration of ATL in the asthma model. Notably, in the *ex vivo* study, OVA-specific T cells treated with splenic DCs were used to specifically clarify the regulatory effect of ATL on DCs (Fig. 4B). However, an i.p. injection of ATL was used in the present study; further studies are warranted to demonstrate the future applications via i.v. or oral administration of ATL.

As DCs serve an important role in the pathogenesis of asthma, therapeutic approaches targeting DCs have been suggested (6). Inhaled corticosteroids, the cornerstone of asthma management, were discovered to decrease the number of DCs in the bronchial mucosa of patients with allergic asthma (32). Using small interfering RNA to knockdown CD80 and CD86 in an OVA-induced asthma murine model, Li *et al* (33) reported that the suppression of CD80/CD86, markers of DCs, decreased the production of IL-4, which is consistent with the results of CD80 in the present study. These findings provided evidence to support the development of medication targeting DCs in allergic diseases, including asthma.

The number of neutrophils in the NC group was abnormally low. While the percentage of neutrophils accounts for >1/2 of total cells in the peripheral blood from normal subjects, it constitutes <1% in BALF under non-inflammatory conditions, which was the primary sample source in the present study (Fig. 1C). In line with the findings of the present study, Heron *et al* (34) reported that the percentages of neutrophils in human peripheral blood mononuclear cells and bronchoalveolar lavage from healthy individuals were ~54.6 and 0.2%, respectively. Similarly, Van Hoecke *et al* (35) described the proportions of murine immune cells in naïve and inflammatory mice and demonstrated that neutrophils in the BALF of naïve mice accounted for <0.1%, whereas this was raised to >80% following lipopolysaccharide stimulation. As a result, it is reasonable to expect a low number of neutrophils in the NC group in the present study.

Based on our previous study (13), it was hypothesized that the mechanisms exerted by ATL on DCs may be associated with the direct suppression of inflammatory cytokines from DCs and the synergistic decrease in the activation of T cells via the downregulation of the MAPK signaling pathway (9,11,13). Additionally, the decrease in inducible nitric oxide synthase was involved in the mechanisms of ATL (36). However, despite the potent bioactivity of ATL, the cytotoxicity induced by ATL in immune cells, particularly DCs, was limited, as evaluated with Cell Counting Kit-8 cell viability assays. Specifically, bone marrow-derived DCs treated with <100 μM ATL exhibited marginal cytotoxicity. The same conclusions were drawn from an animal model experiment in which 40 mg/kg ATL (the same concentration as applied in the present study) was injected into mice, and no significant weight loss was observed (13. Therefore, ATL may be a safe therapeutic option in the management of asthma.

In conclusion, the present study demonstrated that ATL regulated DC maturation, and subsequent Th2 inflammation and AHR in a mouse model of asthma. These results provided evidence that ATL may be a potential therapeutic option for the management of asthma and other allergic diseases involving Th2 inflammation.

Acknowledgements

Not applicable.

Funding

This study was supported by grants from the Changhua Christian Hospital (grant no. 108-CCH-IRP-067) and Animal Biotechnology Center from the Feature Areas Research Center Program of Taiwan Ministry of Education (grant no. MOE-107-S-0023-E).

Availability of data and materials

The datasets generated and/or analyzed in the present study are available from the corresponding author on reasonable request.

Authors' contributions

YCL, WCC and CCL analyzed the data and drafted the manuscript. CCY and TCH contributed to the interpretation of data and revised the manuscript. YCL, WCC and CCL conceived and designed the study. All authors read and approved the final version of the manuscript.

Ethics approval and consent to participate

Ethical approval for the present study was obtained from the IACUC of National Chung-Hsing University (Taichung, Taiwan; approval no. IACUC 108-072).

Patient consent for publication

Not applicable.

Competing interests

The authors declare that they have no competing interests.

References

1. Collaborators GBDCRD; GBD 2015 Chronic Respiratory Disease Collaborators: Global, regional, and national deaths, prevalence, disability-adjusted life years, and years lived with disability for chronic obstructive pulmonary disease and asthma, 1990-2015: A systematic analysis for the Global Burden of Disease Study 2015. Lancet Respir Med 5: 691-706, 2017.
2. Brannan JD: Bronchial hyperresponsiveness in the assessment of asthma control: Airway hyperresponsiveness in asthma: its measurement and clinical significance. Chest 138 (Suppl): 11S-17S, 2010.
3. Wenzel SE: Asthma phenotypes: The evolution from clinical to molecular approaches. Nat Med 18: 716-725, 2012.
4. Simpson JL, Scott R, Boyle MJ and Gibson PG: Inflammatory subtypes in asthma: Assessment and identification using induced sputum. Respirology 11: 54-61, 2006.
5. Cosmi L, Maggi L, Mazzoni A, Liotta F and Annunziato F: Biologicals targeting type 2 immunity: Lessons learned from asthma, chronic urticaria and atopic dermatitis. Eur J Immunol 49: 1334-1343, 2019.
6. Lambrecht BN and Hammad H: The role of dendritic and epithelial cells as master regulators of allergic airway inflammation. Lancet 376: 835-843, 2010.
7. Lambrecht BN and Hammad H: Biology of lung dendritic cells at the origin of asthma. Immunity 31: 412-424, 2009.
8. Xia YG, Yang BY, Wang QH, Liang J, Wang D and Kuang HX: Species classification and quality assessment of cangzhu (*Atractylodis rhizoma*) by high-performance liquid chromatography and chemometric methods. J Anal Methods Chem 2013: 497532, 2013.
9. Jun X, Fu P, Lei Y and Cheng P: Pharmacological effects of medicinal components of *Atractylodes lancea* (Thunb.) DC. Chin Med 13: 59, 2018.
10. Yu C, Xiong Y, Chen D, Li Y, Xu B, Lin Y, Tang Z, Jiang C and Wang L: Ameliorative effects of atractylodin on intestinal inflammation and co-occurring dysmotility in both constipation and diarrhea prominent rats. Korean J Physiol Pharmacol 21: 1-9, 2017.
11. Chae HS, Kim YM and Chin YW: Atractylodin inhibits interleukin-6 by blocking NPM-ALK activation and MAPKs in HMC-1. Molecules 21: 1169, 2016.
12. Tang F, Fan K, Wang K and Bian C: Atractylodin attenuates lipopolysaccharide-induced acute lung injury by inhibiting NLRP3 inflammasome and TLR4 pathways. J Pharmacol Sci 136: 203-211, 2018.
13. Chuang CH, Cheng YC, Lin SC, Lehman CW, Wang SP, Chen DY, Tsai SW and Lin CC: Atractylodin suppresses dendritic cell maturation and ameliorates collagen-induced arthritis in a mouse model. J Agric Food Chem 67: 6773-6784, 2019.
14. National Research Council (US) Committee for the Update of the Guide for the Care and Use of Laboratory Animals: Guide for the Care and Use of Laboratory Animals. 8th edition. National Academies Press (US), Washington, DC, 2011.
15. Lyu Z, Ji X, Chen G and An B: Atractylodin ameliorates lipopolysaccharide and d-galactosamine-induced acute liver failure via the suppression of inflammation and oxidative stress. Int Immunopharmacol 72: 348-357, 2019.
16. Kim SJ, Kim CH, Ahn JH, Kim MS, Kim SC, Lee SY, Kwon SS, Kim YK, Lim KH, Moon HS, *et al*: Time sequence of airway remodeling in a mouse model of chronic asthma: the relation with airway hyperresponsiveness. J Korean Med Sci 22: 183-191, 2007.
17. Padrid P, Snook S, Finucane T, Shiue P, Cozzi P, Solway J and Leff AR: Persistent airway hyperresponsiveness and histologic alterations after chronic antigen challenge in cats. Am J Respir Crit Care Med 151: 184-193, 1995.
18. Chiang CY, Lee CC, Fan CK, Huang HM, Chiang BL and Lee YL: Osthole treatment ameliorates Th2-mediated allergic asthma and exerts immunomodulatory effects on dendritic cell maturation and function. Cell Mol Immunol 14: 935-947, 2017.
19. Weng TY, Li CJ, Li CY, Hung YH, Yen MC, Chang YW, Chen YH, Chen YL, Hsu HP, Chang JY, *et al*: Skin delivery of Clec4a small hairpin RNA elicited an effective antitumor response by enhancing CD8+ immunity in vivo. Mol Ther Nucleic Acids 9: 419-427, 2017.
20. Livak KJ and Schmittgen TD: Analysis of relative gene expression data using real-time quantitative PCR and the 2(-Delta Delta C(T)) method. Methods 25: 402-408, 2001.
21. Kubo M: T follicular helper and TH2 cells in allergic responses. Allergol Int 66: 377-381, 2017.
22. Kumar H, Kim IS, More SV, Kim BW and Choi DK: Natural product-derived pharmacological modulators of Nrf2/ARE pathway for chronic diseases. Nat Prod Rep 31: 109-139, 2014.
23. Zhu F, Du B and Xu B: Anti-inflammatory effects of phytochemicals from fruits, vegetables, and food legumes: A review. Crit Rev Food Sci Nutr 58: 1260-1270, 2018.
24. Schatz M and Rosenwasser L: The allergic asthma phenotype. J Allergy Clin Immunol Pract 2: 645-648, quiz 649, 2014.
25. Choy DF, Hart KM, Borthwick LA, Shikotra A, Nagarkar DR, Siddiqui S, Jia G, Ohri CM, Doran E, Vannella KM, *et al*: TH2 and TH17 inflammatory pathways are reciprocally regulated in asthma. Sci Transl Med 7: 301ra129, 2015.
26. Nials AT and Uddin S: Mouse models of allergic asthma: Acute and chronic allergen challenge. Dis Model Mech 1: 213-220, 2008.
27. Yu QL and Chen Z: Establishment of different experimental asthma models in mice. Exp Ther Med 15: 2492-2498, 2018.
28. Webb DC, Cai Y, Matthaei KI and Foster PS: Comparative roles of IL-4, IL-13, and IL-4Ralpha in dendritic cell maturation and CD4+ Th2 cell function. J Immunol 178: 219-227, 2007.
29. Yi H, Zhang L, Zhen Y, He X and Zhao Y: Dendritic cells induced in the presence of GM-CSF and IL-5. Cytokine 37: 35-43, 2007.
30. Ahn JS and Agrawal B: IL-4 is more effective than IL-13 for in vitro differentiation of dendritic cells from peripheral blood mononuclear cells. Int Immunol 17: 1337-1346, 2005.
31. Roper RL, Conrad DH, Brown DM, Warner GL and Phipps RP: Prostaglandin E2 promotes IL-4-induced IgE and IgG1 synthesis. J Immunol 145: 2644-2651, 1990.

32. Möller GM, Overbeek SE, Van Helden-Meeuwsen CG, Van Haarst JM, Prens EP, Mulder PG, Postma DS and Hoogsteden HC: Increased numbers of dendritic cells in the bronchial mucosa of atopic asthmatic patients: Downregulation by inhaled corticosteroids. Clin Exp Allergy 26: 517-524, 1996.
33. Li JG, Du YM, Yan ZD, Yan J, Zhuansun YX, Chen R, Zhang W, Feng SL and Ran PX: CD80 and CD86 knockdown in dendritic cells regulates Th1/Th2 cytokine production in asthmatic mice. Exp Ther Med 11: 878-884, 2016.
34. Heron M, Grutters JC, ten Dam-Molenkamp KM, Hijdra D, van Heugten-Roeling A, Claessen AM, Ruven HJ, van den Bosch JM and van Velzen-Blad H: Bronchoalveolar lavage cell pattern from healthy human lung. Clin Exp Immunol 167: 523-531, 2012.
35. Van Hoecke L, Job ER, Saelens X and Roose K: Bronchoalveolar lavage of murine lungs to analyze inflammatory cell infiltration. J Vis Exp 4: e55398, 2017.
36. Ishii T, Okuyama T, Noguchi N, Nishidono Y, Okumura T, Kaibori M, Tanaka K, Terabayashi S, Ikeya Y and Nishizawa M: Antiinflammatory constituents of *Atractylodes chinensis* rhizome improve glomerular lesions in immunoglobulin A nephropathy model mice. J Nat Med 74: 51-64, 2020.